JOURNAL OF CATALYSIS **162,** 295–305 (1996)
ARTICLE NO. 0287

Tungsten–Oxo-Species Deposited on Alumina

I. Investigation of the Nature of the Tungstates Deposited on the Interface of the γ-Alumina/Electrolyte Solutions at Various pH's

L. Karakonstantis, K. Bourikas, and A. Lycourghiotis[1]

Department of Chemistry, University of Patras and Institute of Chemical Engineering and High Temperature Chemical Processes, ICE/HT-FORTH, P.O. Box 1414, GR-26500 Patras, Greece

Received October 5, 1995; revised April 5, 1996; accepted April 15, 1996

The mechanism of the deposition of the $W^{(vi)}$ species from aqueous solutions on the γ-alumina surface is refined in this work by investigating critical mechanistic points. A methodology recently developed to investigate the deposition of the $Co^{(II)}$, $Ni^{(II)}$, $Cr^{(VI)}$, and $Mo^{(VI)}$ on γ-alumina has been applied. This methodology is based on the "2p*K*/one site" and "triple-layer" models and involves the writing down of various deposition equilibria, the derivation of the corresponding equations, the calculation of the amount of the deposited $W^{(vi)}$ (through the calculated concentrations of the $W^{(vi)}$ species formed on γ-alumina) at various values of the impregnating parameters, the calculation of the variation, with pH, of the ζ-potential and of the difference in the H^+ ions consumption by the support surface in the presence and absence of the $W^{(vi)}$ species in the impregnating solution. The comparison of the calculated values of the aforementioned parameters with the corresponding ones achieved from deposition experiments, potentiometric titrations, and microelectrophoresis allowed us to establish the mechanism of deposition of $W^{(vi)}$ species on γ-alumina. It was found that although eight different $W^{(vi)}$ species are present in the impregnating solution under the conditions of deposition, the mechanism of deposition was proved to be quite simple:

$$\mathbf{AlOH_2^+ + WO_4^{2-} \longleftrightarrow AlOH_2^+ \ldots WO_4^{2-}} \quad \textbf{[a]}$$

$$\mathbf{AlOH_2^+ + HW_6O_{20}(OH)_2^{5-} \longleftrightarrow AlOH_2^+ \ldots HW_6O_{20}(OH)_2^{5-}} \quad \textbf{[b]}$$

$$\mathbf{AlOH + WO_4^{2-} \longleftrightarrow Al\text{–}O\text{–}(WO_3)^- + OH^-} \quad \textbf{[c]}$$

$$\mathbf{2AlOH + WO_4^{2-} \longleftrightarrow Al\text{–}O\text{–}(WO_2)\text{–}O\text{–}Al + 2OH^-}. \quad \textbf{[d]}$$

According to this mechanism only two $W^{(vi)}$ species contribute to the whole deposition. These species move from the bulk solution to the inner Helmholtz plane (IHP) of the double layer developed between the surface of the support particles and the impregnating solution and then are adsorbed on sites created in the IHP by protonated surface hydroxyl groups of the support. Moreover, the monomeric WO_4^{2-} species, being in the IHP, may react with a single or a pair of adjacent neutral surface hydroxyl groups of the support resulting from the formation of a charged or uncharged $W^{(vi)}$ species, respectively. Lateral intractions are exerted between $W^{(vi)}$ species formed through water molecules also located in the IHP. The study of the variation of the saturation surface concentration of the species illustrated in the rhs of the above equilibria showed that in the pH range 10–6 the deposition occurs practically via reaction (equilibria [c] and [d]). The concentration of Al–O–(WO_2)–O–Al and Al–O–(WO_3^-) species is maximized at pH's 7 and 6, respectively. In the pH range 6–5 both surface reaction and adsorption (equilibria [c] and [a]) contribute to the whole deposition process. The concentration of the $AlOH_2^+ \ldots WO_4^{2-}$ is maximized at pH 5. Finally in the pH range 5–3.5 the deposition takes place exclusively by adsorption (equilibria [a] and [b]). The concentration of the $W^{(vi)}$ species illustrated in the rhs of the second equilibrium is maximized at pH 3.5. The selective deposition of the WO_4^{2-} species with respect to the various polymeric species present in the impregnating suspension was attributed to the relatively low negative charge of these species and the negative potential developed at the IHP.

INTRODUCTION

In a previous article we studied the mechanism of deposition of $W^{(vi)}$–oxo-species on the surface of γ-alumina using deposition experiments, potentiometric titrations, microelectrophoresis, and electron spectroscopy (1). It was inferred that both the protonated and neutral surface hydroxyl groups of the support, but not the deprotonated surface hydroxyl groups, are involved in the deposition of the $H_xW_yO_z(OH)_m^{n-}$ species. It was, moreover, inferred that the adsorption sites are located in the inner Helmholtz plane (IHP) of the electrical double layer developed between the impregnating solution and the surface of the support and that considerable lateral interactions are exerted between the adsorbed tungsten ions. The application of the Stern–Langmuir–Fowler equation to the experimental data allowed for the determination, at various pH's, of the "adsorption constant," the energy of the lateral interactions, as well as of the surface concentration of $W^{(vi)}$ corresponding

[1] To whom correspondence should be addressed.

0021-9517/96 $18.00

to the surface saturation. This concentration increased with decreasing pH taking its maximum value in the pH range 3–4. Moreover, it was inferred that the monomeric (WO_4^{2-}) or oligomeric [$H_xW_yO_z(OH)_m^{n-}$, where $0 < x < 5$, $1 < y < 6$, $4 < z < 22$] tungstates are deposited more easily than the polymeric tungstates.

Although the above study sheds light on the deposition mechanism, some mechanistically important points need elucidation. For instance we do not know either the relative contribution of the neutral and protonated surface hydroxyls to the whole deposition or the concentration of each one of the surface species formed. It is obvious that this information is extremely important for tailoring the preparation of the tungsta-supported γ-alumina catalysts. The goal of the present work is to investigate further the mechanism of the aforementioned deposition and determine the kind and the surface concentration of the $W^{(vi)}$ species formed on the support surface in the pH range 3–10 and at 25°C.

To do the above, we adopted, in general terms, a procedure we recently developed. This procedure applied to elucidating the deposition mechanism in several catalytically important systems (2–4), involving the following steps:

(i) Writing down a very probable mechanistic model based on the findings reported in Ref. (1) and briefly stated above. This model incorporates all the eventualities for the deposition (e.g., deposition through reaction with the neutral surface hydroxyls and adsorption on the protonated surface hydroxyls of different W species as well as reaction and adsorption with different stoichiometries).

(ii) Deriving several equations corresponding to the various deposition equilibria involved in the model.

(iii) Applying a computer program, called SURFEQL (5), to the model. SURFEQL is an interactive code for the calculation of chemical equilibria in aqueous systems. Using this program one may calculate, at 25°C, the equilibrium concentrations of various species being either in the bulk solution or in the solid/liquid interface.

(iv) Testing the proposed deposition model by comparing the experimental curves with the corresponding calculated isotherms for the deposition of $W^{(vi)}$ under various pH's, the calculated difference in the isotherms of hydrogen adsorption on the support surface in the presence and absence of tungstate species, as well as the calculated variation, wiith pH, of the potential at the OHP(Ψ_d), being almost equal to the potential at the shear plane (ζ-potential).

The experimental data used in the present paper have been taken from our previous work presented in Ref. (1). The widely accepted triple-layer model for the double layer and the two p*K*/one-site model for charging the surface mechanism are implied in the present study. In view of the recent development of multisite models for γ-alumina (6–9), the one-site model is of course an approximation, but very useful for modeling complicated depositions in the electrolyte solution/γ-alumina interfaces, where an electrical double layer is developed.

THEORETICAL CONSIDERATIONS

Composition of the Impregnating Solution

In the pH range examined the electrolytic solution contains 12 species (10): {WO_4^{2-}, HWO_4^-, $W_2O_4(OH)^{3-}$, $W_4O_{12}(OH)_4^{4-}$, $HW_4O_{12}(OH)_4^{3-}$, $W_6O_{20}(OH)_2^{6-}$, $HW_6O_{20}(OH)_2^{5-}$, $H_2W_{12}O_{42}^{10-}$, $H_3W_{12}O_{42}^{9-}$, $H_4W_{12}O_{42}^{8-}$, $H_5W_{12}O_{42}^{7-}$, $H_2W_{12}O_{40}^{6-}$}, which are interrelated with the following equilibria:

$$\alpha_1 WO_4^{2-} + \alpha_2 H^+ \overset{K_j}{\longleftrightarrow} H_xW_yO_z(OH)_m^{n-} + \alpha_3 H_2O. \quad [1]$$

These equilibria show that decrease in pH causes an increase in the concentration of the oligomeric and polymeric tungstates at the expense of the WO_4^{2-} ions. The concentration of the various tungstate species at each pH value was calculated from equilibria [1] using SURFEQL. The calculation was based on

$$K_j = \frac{\left[H_xW_yO_z(OH)_m^{n-}\right]}{\left[H_{aq}^+\right]^{\alpha_2}\left[WO_4^{2-}\right]^{\alpha_1}} = \frac{\left[W_{\text{species}_j}^{(vi)}\right]}{[H^+]^{\alpha_2}\left[WO_4^{2-}\right]^{\alpha_1}}. \quad [2]$$

The required K_j values were obtained from the literature (10). It was proved that under our experimental conditions [pH range 10–3,5; concentration range 1.10^{-4}–$2.5\ 10^{-2}$ *M* $W^{(vi)}$] only eight species [WO_4^{2-}($j=1$), HWO_4^- ($j=2$), $W_6O_{20}(OH)_2^{6-}$ ($j=3$), $HW_6O_{20}(OH)_2^{5-}$ ($j=4$), $H_2W_{12}O_{42}^{10-}$ ($j=5$), $H_3W_{12}O_{42}^{9-}$ ($j=6$), $H_4W_{12}O_{42}^{8-}$ ($j=7$), $H_5W_{12}O_{42}^{7-}$ ($j=8$)] are present in considerable extent. Therefore, only these species are considered in the deposition model.

In addition to the $W^{(vi)}$ species, the impregnating solution contains the ions of the indifferent electrolyte, namely NO_3^- and NH_4^+ ions. The latter are hydrolyzed in the solution following the equilibrium

$$NH_3 + H_3O^+ \overset{K_{NH_4^+}}{\longleftrightarrow} NH_4^+ + H_2O. \quad [3]$$

It may be observed that the extent of hydrolysis increases as pH increases. Application of SURFEQL allows one to calculate the concentration of the produced ammonia at each pH. This calculation is based on

$$K_{NH_4^+} = \frac{[NH_4^+]}{[NH_3][H_3O^+]}. \quad [4]$$

Charged Interface

According to the 2p*K*/ one-site model (11, 12), assumed as a good approximation in the present study, the surface

of γ-alumina is charged following

$$AlOH_2^+ \overset{K_1^{int}}{\longleftrightarrow} AlOH + H_s^+ \quad [5]$$

$$AlOH \overset{K_2^{int}}{\longleftrightarrow} AlO^- + H_s^+ \quad [6]$$

$$H_s^+ \longleftrightarrow H_b^+ \quad [7]$$

$$H_2O \longleftrightarrow H_b^+ + OH_b^-. \quad [8]$$

By AlOH, $AlOH_2^+$, and AlO^- we denote, respectively, neutral, protonated, and deprotonated surface hydroxyls. K_1^{int} and K_2^{int} represent the surface acidity constants. The subscripts s and b stand for the surface and bulk solution, respectively. Equilibria [5]–[7] are described by

$$K_1^{int} = \frac{[H_s^+][AlOH]}{[AlOH_2^+]} \quad [9]$$

$$K_2^{int} = \frac{[AlO^-][H_s^+]}{[AlOH]} \quad [10]$$

$$[H_s^+] = [H_b^+]\exp\left(-\frac{F\Psi_0}{RT}\right). \quad [11]$$

In Eq. [11], Ψ_0 denotes the Volta potential at the surface.

The values of the surface acidity constants have been determined using potentiometric titrations (11). These values do not change due to the presence of the tungstate species in the impregnating solution. Therefore, they may be used to determine, using SURFEQL, the concentration of the various types of surface hydroxyls at each pH both in the absence and presence of the $W^{(vi)}$ species.

To accomplish the description of equilibria taking place even in the absence of the $W^{(vi)}$ species in the impregnating solution, it should be noted that previous studies have shown that only the NH_4^+ ions of the NH_4NO_3 used as background electrolyte can be adsorbed on sites, on the IHP, created by the deprotonated surface hydroxyls of γ-alumina (4):

$$NH_4^+ + AlO^- \overset{\bar{K}_{NH_4^+}}{\longleftrightarrow} AlO^- \ldots NH_4^+. \quad [12]$$

The constant of this equilibria is given by

$$\bar{K}_{NH_4^+} = \frac{[AlO^- \ldots NH_4^+]}{[NH_4^+]_{IHP}[AlO^-]}. \quad [13]$$

The subscript IHP in the above equation takes into account that the NH_4^+ illustrated in the left-hand side (lhs) of equilibrium [12] are considered to be located in the IHP. To obtain the value of $[NH_4^+]_{IHP}$ we may use an expression analogous to Eq. [11], which relates the concentration of the ammonium ion in the bulk solution, $[NH_4^+]_b$, with that in the IHP.

$$[NH_4^+]_{IHP} = [NH_4^+]_b \exp\left(-\frac{F\Psi_{IHP}}{RT}\right). \quad [14]$$

Deposition Model

In view of our results reported in Ref. (1) and the findings concerning the composition of the impregnating suspension under our experimental conditions stated above it seems reasonable to start approaching the real deposition mechanism, by testing the following quite general model:

$$AlOH_{2(surf)}^+ + W^{(vi)}\ species_{j(IHP)} \longleftrightarrow AlOH_{2(surf)}^+ \ldots W^{(vi)}\ species_{j(IHP)} \quad [15]$$

$$2AlOH_{2(surf)}^+ + W^{(vi)}\ species_{j(IHP)} \longleftrightarrow (AlOH_2^+)_{2(surf)} \ldots W^{(vi)}\ species_{j(IHP)} \quad [16]$$

$$AlOH_{(surf)} + W^{(vi)}\ species_{j(IHP)} \longleftrightarrow Al\text{–}O_{(surf)}\text{–}W^{(vi)}\ species_{j(IHP)} + OH_{(IHP)}^- \quad [17]$$

$$2AlOH_{(surf)} + W^{(vi)}\ species_{j(IHP)} \longleftrightarrow Al\text{–}O_{(surf)}\text{–}W^{(vi)}\ species_{j(IHP)}\text{–}O_{(surf)}\text{–}Al + 2OH_{(IHP)}^- \quad [18]$$

$$AlOH_{2(surf)}^+ + AlOH_{(surf)} + W^{(vi)}\ species_{j(IHP)} \longleftrightarrow Al\text{–}OH_{2(surf)}^+ \ldots W^{(vi)}\ species_{j(IHP)}\text{–}O_{(surf)}\text{–}Al + OH_{(IHP)}^-. \quad [19]$$

According to the above model a $W^{(vi)}$ species, being in the impregnating solution in a remarkable concentration, first moves to the IHP and then is adsorbed on a site in this plane created by one or two protonated surface hydroxyls (equilibria [15], [16]). Adsorption on a site created by more than two protonated hydroxyls is not a realistic assumption. For example studies devoted to the adsorption of molybdates (3) or chromates (4) on the γ-alumina surface have shown negligible adsorption, if any, of the $Mo^{(vi)}$ or $Cr^{(vi)}$ species even on a site created by two protonated surface hydroxyls. It should be noted that the $W^{(vi)}$ species illustrated in the lhs of equilibria [15]–[19] are considered to be in the IHP. Moreover, for the species HWO_4^- with charge lower than two, we do not consider adsorption on a site created by two protonated surface hydroxyls. According to the above model the tungstate species, being in the IHP, may be deposited, moreover, by reaction with the neutral surface hydroxyls, providing the surface complexes illustrated in equilibria [17], [18]. Finally the tentative model proposed postulates that the deposition of the $W^{(vi)}$ species may take place by both processes: adsorption on a site created by one $AlOH_2^+$ group and reaction with one AlOH group (equilibrium [19]). Taking into account the above as well as the fact that different species are present in the impregnating solution, it is clear that the above equation describes more than

five equilibria. It may be easily calculated that the above equations describe 37 different equilibria. Equations [15], [16], [17], [18], and [19] describe respectively equilibria 1–8, 9–15, l6–23, 24–30, and 31–37.

Derivation of Equations for Describing the Deposition Equilibria

Following a procedure similar (but not identical) with that described in Ref. (4), a generalization of which has been recently achieved [13], we may derive

$$C_i = \lambda_l^{-1}\exp\left(-\frac{\Delta G^0_{CS,i}}{RT}\right)\exp\left(\frac{\mu_i F\varphi_0}{RT}\right)10^{\nu_i(14-\mathrm{pH})} \times \exp\left(\frac{|z_i|F\Psi_{\mathrm{IHP}}}{RT}\right)\exp\left(\frac{b_i g_i \overline{E} n\Gamma}{\sum_{i=1}^{37} b_i g_i \Gamma_m RT}\right) \times \left[\mathrm{W^{(vi)}\ species}_j\right]_b \left(C^{\mathrm{f}}_{\mathrm{AlOH}_2^+}\right)^{\mu_i}\left(C^{\mathrm{f}}_{\mathrm{AlOH}}\right)^{\nu_i}. \quad [20]$$

The subscript i corresponds to a given equilibrium. A supported $W^{(vi)}$ species formed through an equilibrium i is denoted as $W^{(vi)}$ species$_i$. In the above equation by C_i, $\Delta G^0_{CS,i}$, μ_i, F, φ_0, ν_i, b_i, g_i, $\overline{E}$, n, Γ, Γ_m, $[W^{(vi)}\ \mathrm{species}_j]_b$, $C^{\mathrm{f}}_{\mathrm{AlOH}_2^+}$, and $C^{\mathrm{f}}_{\mathrm{AlOH}}$ we symbolize, respectively, the concentration of a $W^{(vi)}$ species$_i$ illustrated in the rhs of Eqs. [15]–[19], the standard free energy of the chemical interactions between the deposited $W^{(vi)}$–oxo-species and the sites of the support for an equilibrium i, the number of the $AlOH_2^+$ groups involved in the equilibrium i, the Faraday constant, the Galvani potential at the surface, the number of AlOH groups involved in the equilibrium i, a "structural" factor defined by the sum [number of W–O bonds $+ 2|z_i|$], where z_i represents the charge of $W^{(vi)}$ species$_i$, a concentration factor equal to $1/|\log C_i|$, where C_i represents the concentration of a $W^{(vi)}$ species$_i$ calculated initially, the mean energy of the lateral interactions exerted between the deposited $W^{(vi)}$ species, the number of the kind of the $W^{(vi)}$ species that are formed on the support surface at a given pH, the surface and the saturation surface concentration of the aforementioned species, the concentration of the $W^{(vi)}$ species in the bulk solution at equilibrium, and the concentration of the uncovered (free) $AlOH_2^+$ and AlOH groups. λ_i is a proportionality constant (13).

Unfortunately, Eq. [20] cannot by used directly for the calculation of the concentration of a $W^{(vi)}$ species$_i$ formed on the support surface, for two main reasons. First, the product of the first four terms of Eq. [20] are unknown. However, this product is constant at a constant pH. Therefore, we may write the relationship

$$K_i = \lambda_i^{-1}\exp\left(-\frac{\Delta G^0_{CS,i}}{RT}\right)\exp\left(\frac{\mu_i F\phi_0}{RT}\right)10^{\nu_i(14-\mathrm{pH})}, \quad [21]$$

where K_i is the deposition constant for the $W^{(vi)}$ species$_i$ formed on the support surface. This constant describes the deposition from the IHP to the "final deposition state." The second reason is that the mean energy of the lateral interactions exerted between the deposited $W^{(vi)}$ species, $\overline{E}$, is also unknown. It is therefore necessary to adopt an approximate procedure to determine the values of K_i and $\overline{E}$ and then return and use Eq. [20]. This can be achieved by deriving an approximate equation that would be tested experimentally. The derivation of this expression is achieved following a procedure similar, but not identical, with that described in Ref. (4), a generalization of which has been recently achieved [13]. Only the most important points are presented here, The starting point is the following:

$$\frac{\Theta_i}{\left(1-\Theta_{\mathrm{AlOH}_2^+}\right)^{\mu_i}\left(1-\Theta_{\mathrm{AlOH}}\right)^{\nu_i}} = \exp\left(-\frac{\Delta G^0_{CS,i}}{RT}\right)\exp\left(\frac{\mu_i F\varphi_0}{RT}\right)10^{\nu_i(14-\mathrm{pH})} \times \exp\left(\frac{|z_i|F\Psi_{\mathrm{IHP}}}{RT}\right)\cdot\exp\left(\frac{E_i\Gamma}{\Gamma_m RT}\right)[W^{(vi)}\ \mathrm{species}_j]_b. \quad [22]$$

In the above equation, by Θ_i, $\Theta_{\mathrm{AlOH}_2^+}$, and Θ_{AlOH} symbolize, respectively, the fraction of the sites covered by the $W^{(vi)}$ species$_i$, the fraction of covered $AlOH_2^+$ groups, and the fraction of the AlOH groups. These fractions are defined by the following:

$$\Theta_i = \lambda_i \frac{C_i}{\left(C^{\mathrm{t}}_{\mathrm{AlOH}_2^+}\right)^{\mu_i}\left(C^{\mathrm{t}}_{\mathrm{AlOH}}\right)^{\nu_i}}, \quad [23]$$

$$\Theta_{\mathrm{AlOH}_2^+} = \frac{C^{\mathrm{c}}_{\mathrm{AlOH}_2^+}}{C^{\mathrm{t}}_{\mathrm{AlOH}_2^+}}, \quad [24]$$

$$\Theta_{\mathrm{AlOH}} = \frac{C^{\mathrm{c}}_{\mathrm{AlOH}}}{C^{\mathrm{t}}_{\mathrm{AlOH}}}, \quad [25]$$

In the above equations, the superscripts t and c denote, respectively, total (covered + uncovered) and covered hydroxyl groups. λ_i is a proportionality constant.

The derivation of the desired approximate expression can be achieved on the basis of the following assumptions:

(i) K_i involves the term $\exp(|z_i|F\Psi_{\mathrm{IHP}}/RT)$, which describes the transport of the $W^{(vi)}$ species$_j$ from the bulk solution into IHP.

(ii) $E_i \approx \overline{E}$.

(iii) $\sum_{i=1}^{37} \frac{\Theta_i}{\left(1-\Theta_{\mathrm{AlOH}_2^+}\right)^{\mu_i}\left(1-\Theta_{\mathrm{AlOH}}\right)^{\nu_i}} \approx \frac{\Theta}{1-\Theta}$,

where Θ represents the fraction of the sites covered by the

$W^{(vi)}$ species illustrated in the rhs of equilibria, which are described by Eq. [15]–[19].

(iv) $[W^{(vi)}\text{species}_j]_b = \alpha_j [W^{(vi)}]_t = \alpha_j C_{eq}$, where $[W^{(vi)}]_t = C_{eq}$ represents the total concentration of the impregnating solution in $W^{(vi)}$ at equilibrium and α_j a coefficient nearly independent of C_{eq}.

Taking into account the above approximations we may add Eqs. [22] and obtain the approximate equation

$$\frac{\Theta}{1-\Theta} = \overline{K} C_{eq} \exp\left(\frac{\overline{E}\Gamma}{\Gamma_m RT}\right). \quad [26]$$

Taking into account that $\Theta \equiv \Gamma/\Gamma_m$, Eq. [26] may be easily transformed into

$$\frac{1}{\Gamma} = \frac{1}{\Gamma_m} + \frac{1}{\overline{K}\Gamma_m C_{eq} \exp(\overline{E}\Gamma/\Gamma_m RT)}. \quad [27]$$

Obviously Eq. [27] can be tested experimentally, because it predicts a linear dependence of $1/\Gamma$ on $1/C_{eq}\exp(\overline{E}\Gamma/\Gamma_m RT)$. Both Γ and C_{eq} are determined experimentally. The deposition constant $\overline{K}$ is given by

$$\begin{aligned}\overline{K} &= (p_1\alpha_1 + p_2\alpha_2 + p_3\alpha_3 + p_4\alpha_4 + p_5\alpha_5 + p_6\alpha_6 + p_7\alpha_7 + p_8\alpha_8)K_a \\ &+ \left(p_1^2\alpha_1 + p_3^2\alpha_3 + p_4^2\alpha_4 + p_5^2\alpha_5 + p_6^2\alpha_6 + p_7^2\alpha_7 + p_8^2\alpha_8\right)K_a^2 \\ &+ (\alpha_1 + \alpha_2 + \alpha_3 + \alpha_4 + \alpha_5 + \alpha_6 + \alpha_7 + \alpha_8)K_c\, 10^{(14-\text{pH})} \\ &+ (\alpha_1 + \alpha_3 + \alpha_4 + \alpha_5 + \alpha_6 + \alpha_7 + \alpha_8)K_c^2\, 10^{2(14-\text{pH})} \\ &+ (p_1\alpha_1 + p_3\alpha_3 + p_4\alpha_4 + p_5\alpha_5 + p_6\alpha_6 + p_7\alpha_7 + p_8\alpha_8) \\ &\qquad \cdot K_a K_c\, 10^{(14-\text{pH})}. \quad [28]\end{aligned}$$

In the above equation p_i represents the ratio of the protonation constant of a $W^{(vi)}$ species illustrated in the lhs of an equilibrium i to that of the WO_4^{2-} ions.

The constants K_a and K_c involved in the above equation are related with the constants K_i of the equilibria 1–37 by the following:

$$K_a \equiv \frac{K_i}{p_i}, \quad i = 1, 2, 3, 4, 5, 6, 7, \text{and } 8 \quad [29]$$

$$K_a^2 = K_b \equiv \frac{K_i}{p_i}, \quad i = 9, 10, 11, 12, 13, 14, \text{and } 15 \quad [30]$$

$$K_c \equiv \frac{K_i}{10^{(14-\text{pH})}}, \quad i = 16, 17, 18, 19, 20, 21, 22, \text{and } 23 \quad [31]$$

$$K_c^2 = K_d \equiv \frac{K_i}{10^{(28-2\text{pH})}}, \quad i = 24, 25, 26, 27, 28, 29, \text{and } 30 \quad [32]$$

$$\frac{K_a K_c}{p_i} = K_e \equiv \frac{K_i}{10^{(14-\text{pH})}}, \quad i = 31, 32, 33, 34, 35, 36, \text{and } 37 \quad [33]$$

Calculations in the Impregnating Solutions for Obtaining the Values of α_j

Values of the protonation constants drawn from the literature allowed us to determine the values of p_i.

The values of K_j obtained from the literature (10) and a guessing value for the $[WO_4^{2-}]$ are inserted into the SURFEQL and the values of $[W^{(vi)}\ \text{species}_j]_b$ ($j = 2$–8) are calculated at each pH. The calculations are based on Eq. [2]. The calculating process is repeated automatically for various conjectured values of $[WO_4^{2-}]$ until a satisfaction of the relationship [34] to be achieved:

$$\begin{aligned}&[WO_4^{2-}] + [HWO_4^-] + 6\left[W_6O_{20}(OH)_2^{6-}\right] \\ &\quad + 6\left[HW_6O_{20}(OH)_2^{5-}\right] + 12\left[H_2W_{12}O_{42}^{10-}\right] \\ &\quad + 12\left[H_3W_{12}O_{42}^{9-}\right] + \left[12H_4W_{12}O_{42}^{8-}\right] \\ &\quad + 12\left[H_5W_{12}O_{42}^{7-}\right] = [W^{(vi)}]_t, \quad [34]\end{aligned}$$

where $[W^{(vi)}]_t$ represents the total concentration of the $W^{(vi)}$ in the solution. A similar procedure based on Eq. [4] was followed by calculating the concentration of NH_4^+ and NH_3 in the impregnating solution at various pH's. Using the above calculated values for the $[W^{(vi)}\ \text{species}_j]_b$ we calculate the values of α_j. This calculation is based on the relation $[W^{(vi)}\ \text{species}_j]_b = \alpha_j C_{eq}$ assumed before.

Calculations in the Impregnating Suspensions and Elucidation of the Deposition Mechanism

The values of $\overline{K}$, $\overline{E}$, and Γ_m are determined by applying Eq. [27] to the experimental deposition data. As already mentioned a plot of $1/\Gamma$ vs $1/C_{eq}\exp(\overline{E}\Gamma/\Gamma_m RT)$ should provide a straight line for a proper value of $\overline{E}$. Figure 4 of Ref. (1) illustrates some typical results.

The determined values of p_i and α_j are inserted into Eq. [28]. This allows us to select a pair of values for K_a and K_c which, at a given pH, render the rhs of Eq. [28] equal to the experimentally determined value of $\overline{K}$.

The so selected values of K_a and K_c are used to calculate a set of *initial* values for K_i and then for the amount $K_i \exp(\overline{E}\Gamma/\Gamma_m RT)10^{-\nu_i(14-\text{pH})}$ ($i = 1$–37, see Eqs. [29]–[33]).

The values for the amount $K_i \exp(\overline{E}\Gamma/\Gamma_m RT)10^{-\nu_i(14-\text{pH})}$ as well as values for the parameters illustrated in Table 1 are inserted into SURFEQL. Specifically, the following parameters should be inserted into the program: (i) the values of SSA, *SC*, C_1, and C_2; (ii) conjectured values for [AlOH], $[WO_4^{2-}]_b$, and $[NH_4^+]$; (iii) the values of K_1^{int} and K_2^{int}. At this point it should be noted that the values of K_1^{int} and K_2^{int} of the equilibria [9] and [10] have been determined by potentiometric titration in the absence of the tungstate species in the impregnating suspension. The methodology followed has been reported elsewhere (2). In this calculating step it is tentatively assumed that $\exp(-F\Psi_{IHP}/RT) = \exp(-F\Psi_0/RT) = \exp(-F\Psi_d/RT) = 1$.

Starting with the conjectured guessing values, the program runs by solving the system of the various mass action law equations mentioned in the text; among those the most important is Eq. [20], as well as mass and charge balance

TABLE 1

Parameters Required for the Application of SURFEQL to the Proposed Model

Parameter	Symbol	Value	Units	Reference
Total surface sites density	N_s	8	Sites nm^{-2}	(2)
Deprotonation constant of the $AlOH_2^+$ groups	K_1^{int}	$10^{-3.87}$		(2)
Deprotonation constant of the AlOH groups	K_2^{int}	$10^{-7.41}$		(2)
Constants of equilibria 1 corresponding to $W^{(vi)}$ species$_j$, $j=2$–8	K'_j $j=2$–8	$10^{2.5}$, $10^{52.08}$, $10^{60.17}$, $10^{128.24}$, $10^{129.52}$, $10^{134.79}$, $10^{138.39}$		
Total $W^{(vi)}$ concentration	$[W^{(vi)}]_t$		mol dm^{-3}	
Total NH_4^+ and NO_3^- concentrations	$[NH_4^+]_t$ $[NO_3^-]_t$		mol dm^{-3}	
pH	pH			
Specific surface area	SSA	123	m^2 g^{-1}	(1)
Solid concentration	SC	3.57	g dm^{-3}	(1)
Ionic strength	I	0.16	mol dm^{-3}	(1)
Inner capacitance	C_1	9.9	F m^{-2}	
Outer capacitance	C_2	0.2	F m^{-2}	

equations similar to those illustrated in (4, Appendix 2) or in (13). This allows the calculation of the concentration values for all the species involved in the various equilibria presented in the text as well as the values of the electrical parameters illustrated in Table 2. Among these parametrs the most important are the values of C_i ($i=1$–37), namely the values for the concentration of each $W^{(vi)}$ species$_i$ formed on the support surface (see Eq. [20]). From the values of C_i, the values of Γ_i (surface concentration for a $W^{(vi)}$ species$_i$) are calculated. These Γ_i values are considered as initial ones because the term $K_i \exp(\overline{E}\Gamma/\Gamma_m RT)10^{-\nu_i(14-pH)}$ instead of the term $K_i \exp(b_i g_i \overline{E} n\Gamma/\sum_{i=1}^{37} b_i g_i \Gamma_m RT)10^{-\nu_i(14-pH)}$, which is unknown for the moment, had been considered to be involved in Eq. [20]. From the initial values of Γ_i, we calculate the value of Γ, namely the surface concentration of the deposited $W^{(vi)}$. Therefore, the depositon isotherms Γ vs C_{eq} may be calculated and compared with the corresponding ones achieved experimentally. The calculation procedure is repeated many times for various values of K_a, K_c satisfying Eq. [28] until the optimum pair K_a, K_c is achieved. However, even for this pair the agreement achieved between the calculated and experimental Γ vs C_{eq}. curves is not sufficient in most cases (see Fig. 1). Nevertheless, this calculating step allowed us to detemine the initial values of Γ_i and then

TABLE 2

Parameters or Variables Derived from the Application of SURFEQL to the Proposed Model

Parameter	Symbol	Units
Surface charge density	σ_0	C m^{-2}
Charge density at the IHP	σ_1	C m^{-2}
Charge density at the OHP	σ_d	C m^{-2}
Surface potential	Ψ_0	V
Potential at the IHP	Ψ_{IHP}	V
Potential at the OHP	Ψ_d	V
Equilibrium concentration of H^+	$[H^+]_b$	mol dm^{-3}
Equilibrium concentration of the $W^{(vi)}$ species$_j$ in the solution	$[W^{(vi)}\ species_j]_b$ $j=1$–8	mol dm^{-3}
Equilibrium concentration of NH_4^+ (NO_3^-)	$[NH_4^+]_b$ ($[NO_3^-]_b$)	mol dm^{-3}
Equilibrium concentration of the $W^{(vi)}$ species illustrated in the right-hand side of Eqs. [15]–[19]	$W^{(vi)}\ species_i]_{surf\text{-}IHP}$ or C_i, $i=1$–37	mol dm^{-3}
Equilibrium concentration of AlOH	[AlOH] or C_{AlOH}	mol dm^{-3}
Equilibrium concentration of $AlOH_2^+$	$[AlOH_2^+]$ or $C_{AlOH_2^+}$	mol dm^{-3}
Equilibrium concentration of AlO^-	$[AlO^-]$ or C_{AlO^-}	mol dm^{-3}

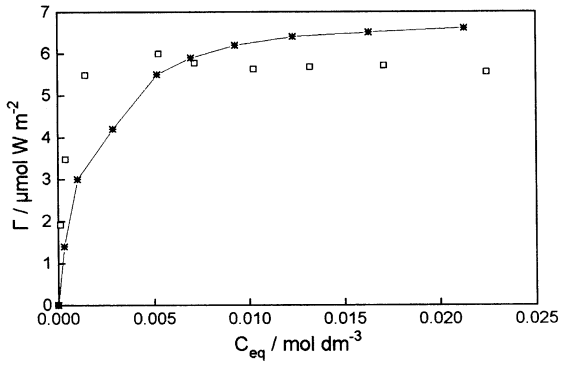

FIG. 1. Variation of the surface concentration of $W^{(vi)}$ with equilibrium $W^{(vi)}$ concentration: experimental (□) and calculated (∗) isotherm for the total W deposition. pH 6.4l, $T = 25°C$, $I = 0.16\ M\ NH_4NO_3$.

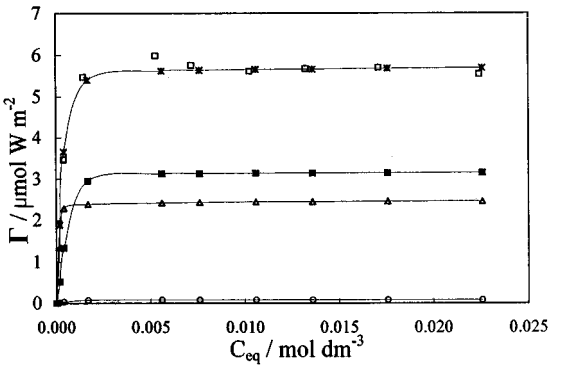

FIG. 2. Variation of the surface concentration of $W^{(vi)}$ with equilibrium $W^{(vi)}$ concentration: experimental (□) and calculated (∗) isotherm for the total W deposition. Symbols correspond to the calculated isotherms of the surface species: (○) $AlOH_2^+ \ldots WO_4^{2-}$, (■) Al–O–$(WO_3)^-$, and (△) Al–O–$(WO_2)$–O–Al. pH 6.41, $T = 25°C$, $I = 0.16\ M\ NH_4NO_3$.

the values of the concentration factor g_i ($g_i = 1/|\log C_i|$). Moreover, at the end of this calculating step we know which postulated equilibria contribute practically to the whole deposition. In other words we know which equilibria provide nonnegligible values of Γ_i over the C_{eq} range. Therefore, the value of n at a given pH may be calculated. Finally, the knowledge of the equilibria that practically contribute to the whole deposition at a given pH allows the modification of Eq. [28] by eliminating from it the terms that are related with the equilibria with negligible contribution.

Starting with the optimum value for K_a we recalculate the value of K_c using the proper expression of Eq. [28] at a given pH. The so determined values of K_a, K_c, g_i, and n are used to determine the corresponding values for the amount $K_i \exp(b_i g_i \overline{E} n\Gamma / \sum_{i=1}^{37} b_i g_i \Gamma_m RT) 10^{-\nu_i(14-\mathrm{pH})}$. These values are inserted into SURFEQL together with the values for the parameters illustrated in Table 1. The calculating procedure mentioned before is repeated. After a few runs for various K_a, K_c values a good agreement between the calculated and experimental Γ vs C_{eq} is achieved. A typical example is illustrated in Fig. 2. It is worth noting that there is only one pair of (K_a, K_c) at each pH that provides this very good agreement. The possibility of finding this unique pair of K_a, K_c for achieving the aforementioned agreement depends on the postulated mechanism. Thus, the assumption of an "incorrect" mechanistic model does not permit the selection of any set of Equilibrium constants to achieve an agreement between the calculated and the experimental curve Γ vs C_{eq}.

Testing of the Selected Mechanism

It is obvious that the ability of the support to adsorb hydrogen ions should be influenced by the presence of the $W^{(vi)}$ species in the impregnating solution. In fact, it was found that the amount of H^+ ions consumed on the γ-alumina surface (see equilibria 5–8) as a function of the pH of the suspension is different in the absence and presence of the $W^{(vi)}$ species in the suspension [see (1, Fig. 10)]. It is expected that the magnitude of this effect should depend on the deposition mechanism.

As may be observed in Table 2, using SURFEQL we may calculate at each pH the difference in the presence and absence of the $W^{(vi)}$ species$_j$ in the suspension in the amount $(AlOH_2^+ – AlO^-)_t$ (t stands for the total covered and uncovered groups). This is denoted by $\Delta(AlOH_2^+ – AlO^-)_t$. On the other hand using potentiometric titrations we may determine the variation, with pH, in the difference of hydrogen ions consumed in equilibria 5–8 in the presence and absence of the $W^{(vi)}$ species$_j$ in the suspension. This is denoted by ΔH_c^+ and may be easily achieved by subtracting curve (a) from curve (b) illustrated in (1, Fig. 10). It is obvious that if the proposed model describes indeed the deposition process the variation $\Delta(AlOH_2^+ – AlO^-)_t$ vs pH and ΔH_c^+ vs pH must be identical. The very good agreement achieved is illustrated in Fig. 3. This agreement corroborates the postulated mechanism.

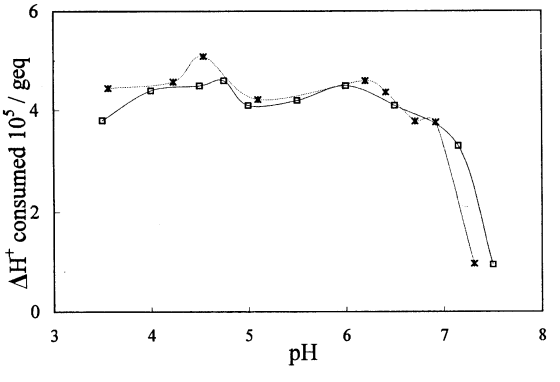

FIG. 3. Variations, with pH, in the differences (in the presence and absence of $W^{(vi)}$ species$_j$ in the impregnating suspension) of the hydrogen ions consumed on the surface of γ-alumina, ΔH_c^+ (□), as well as of the "total protonated minus total deprotonated surface hydroxyls," $\Delta\ (AlOH_2^+ – AlO^-)$ (∗) $T = 25°C$, $I = 0.16\ M\ NH_4NO_3$.

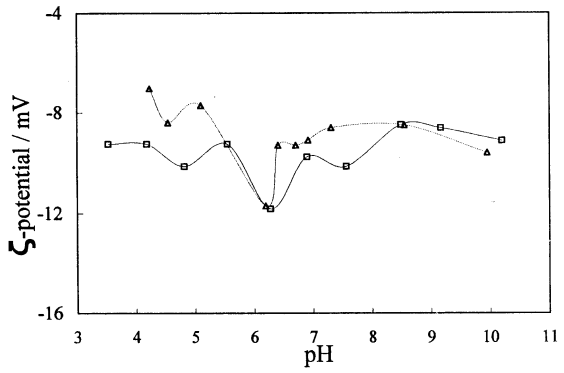

FIG. 4. The variation, with pH, of the ζ-potential in the presence of $W^{(vi)}$ species: (□) experimental values; (△) calculated values. $T = 25°C$, $I = 0.01\ M\ NH_4NO_3$.

In Table 2 it may be seen that using SURFEQL we may calculate the Volta potential at the shear plane of the double layer, Ψ_d, assumed approximately equal to the ζ-potential determined by microelectrophoretic mobility measurements. Figure 4 illustrates the variation with pH of the ζ-potential calculated by SURFEQL (Δ) and determined experimentally in the presence of the $W^{(vi)}$ species$_j$ in the suspension (□). Very good agreement is achieved, which corroborates the postulated mechanism.

RESULTS AND DISCUSSION

The Real Deposition Mechanism

Following the procedure described in the previous two sections we found that the general mechanism assumed in the Introduction describes our deposition data. This allowed us to calculate, over the whole pH range studied, the concentration of each of the $W^{(vi)}$ species$_i$ illustrated in the rhs of Eqs. [15]–[19] (equilibria 1–37) and plot the corresponding isotherms. An example, for pH 6.41, is illustrated in Fig. 2, where the calculated isotherms corresponding to equilibria [a], [c], and [d] can be seen. In this pH the other equilibria do not practically contribute to the deposition and this is the reason for the corresponding calculated isotherms not being illustrated. The careful inspection of the calculated isotherms for all species illustrated in the rhs of equilibria 1–37 in the pH range 4.23–9.95 *demonstrated that only the equilibria* [*a*], [*b*], [*c*], and [*d*] *contribute practically to the whole deposition.* Consequently the deposition mechanism assumed in the Introduction may be significantly simplified into

$$AlOH_2^+ + WO_4^{2-} \longleftrightarrow AlOH_2^+ \ldots WO_4^{2-} \quad [a]$$

$$AlOH_2^+ + HW_6O_{20}(OH)_2^{5-} \longleftrightarrow AlOH_2^+ \ldots HW_6O_{20}(OH)_2^{5-} \quad [b]$$

$$AlOH + WO_4^{2-} \longleftrightarrow Al\text{–}O\text{–}(WO_3)^- + OH^- \quad [c]$$

$$2AlOH + WO_4^{2-} \longleftrightarrow Al\text{–}O\text{–}(WO_2)\text{–}O\text{–}Al + 2OH^-. \quad [d]$$

This is the most important finding of the present work. In Ref. (1) we noted the participation of the neutral surface hydroxyls, in addition to the protonated ones, in the whole deposition process. However, the level of sophistication of our computational methodology in that time did not allow us to understand how important is the chemical reaction as a deposition process at relatively high pH values. Therefore, from this respect, the present work offers a deeper understanding concerning the deposition of the $W^{(vi)}$–oxo-species on the γ-alumina surface. Although the selected mechanism is supported on three independent experimental tests performed in a wide pH range, the complex chemistry of the $W^{(vi)}$ species in the bulk solution and the lack of a large number of experimental points on the deposition isotherms justify some kind of uncertainty. The main reasons for the other equilibria not contributing to the whole deposition are discussed in the next section.

Let us return to the aforementioned simplified mechanism. The relative contribution of the equilibria [a], [b], [c], and [d] to the whole deposition of $W^{(vi)}$ on the γ-alumina surface is illustrated in Fig. 5. In all cases the concentration of the deposited $W^{(vi)}$ corresponds to the plateau of the calculated isotherms. It may be seen that in the pH range 10–5 the only $W^{(vi)}$ species deposited on the γ-alumina surface is the monomeric WO_4^{2-} ions. In fact, a decrease in pH below this value is required for the polymeric $HW_6O_{20}(OH)_2^{5-}$ to contribute significantly to the deposition. However, at the lowest pH examined the contribution to the whole $W^{(vi)}$ deposition, expressed in moles of the deposited species, of the WO_4^{2-} still remains considerable. Another interesting observation is that in the pH range 6–10 deposition takes

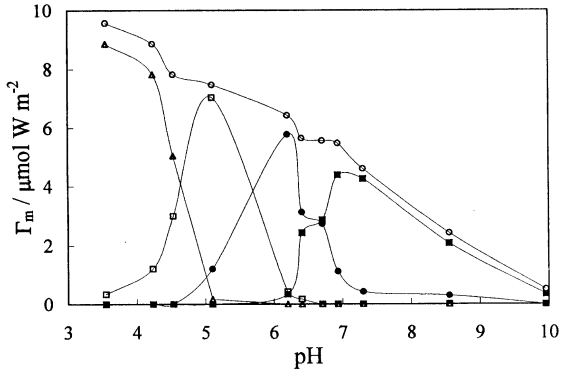

FIG. 5. Variation, with pH, of the maximum amount of $W^{(vi)}$ deposited through adsorption of one WO_4^{2-} ion on a site created by one $AlOH_2^+$ group (□), through adsorption of one $HW_6O_{20}(OH)_2^{5-}$ ion on a site created by $AlOH_2^+$ group (△), through reaction of the WO_4^{2-} ion with a AlOH group (●) and through reaction of WO_4^{2-} ion with a pair of adjacent AlOH groups (■), The variation of the Γ_m with pH for the total amount of the deposited $W^{(vi)}$ is also indicated (○). $T = 25°C$, $I = 0.16\ M\ NH_4NO_3$.

TABLE 3

Compiles the Values of the Concentration of the $W^{(vi)}$ $Species_j$ in the Bulk Solution[a]

Species (pH)	3.56	4.23	4.54	5.10	6.20	6.41	6.71	6.92	7.31	8.55	9.95
$[WO_4^{2-}]_b$	1.36×10^{-7}	1.09×10^{-6}	2.16×10^{-6}	1.24×10^{-5}	2.10×10^{-4}	3.14×10^{-4}	9.14×10^{-4}	1.79×10^{-3}	3.98×10^{-3}	2.00×10^{-2}	2.00×10^{-2}
$[HWO_4^{-}]_b$	6.54×10^{-8}	9.29×10^{-8}	1.03×10^{-7}	1.34×10^{-7}	2.00×10^{-7}	2.13×10^{-7}	2.47×10^{-7}	2.71×10^{-7}	3.02×10^{-7}	9.59×10^{-8}	3.03×10^{-9}
$[W_2O_7(OH)^{3-}]_b$	3.71×10^{-12}	4.21×10^{-11}	9.28×10^{-11}	6.91×10^{-10}	1.82×10^{-8}	2.78×10^{-8}	9.37×10^{-8}	2.01×10^{-7}	5.00×10^{-7}	7.98×10^{-7}	2.52×10^{-8}
$[W_4O_{12}(OH)_4^{4-}]_b$	1.04×10^{-22}	4.26×10^{-22}	6.55×10^{-22}	1.82×10^{-21}	9.23×10^{-21}	1.17×10^{-20}	2.11×10^{-20}	3.08×10^{-20}	4.78×10^{-20}	4.84×10^{-22}	4.84×10^{-28}
$[HW_4O_{12}(OH)_4^{3-}]_b$	3.02×10^{-22}	2.19×10^{-22}	1.90×10^{-22}	1.18×10^{-22}	5.29×10^{-23}	4.78×10^{-23}	3.44×10^{-23}	2.82×10^{-23}	2.19×10^{-23}	1.40×10^{-26}	4.43×10^{-34}
$[W_4O_{20}(OH)_2^{6-}]_b$	4.63×10^{-10}	3.81×10^{-9}	7.28×10^{-9}	3.37×10^{-8}	3.85×10^{-7}	5.49×10^{-7}	1.33×10^{-6}	2.35×10^{-6}	4.54×10^{-6}	4.62×10^{-9}	4.62×10^{-18}
$[HW_6O_{20}(OH)_2^{5-}]_b$	4.99×10^{-7}	7.30×10^{-7}	7.84×10^{-7}	8.12×10^{-7}	8.21×10^{-7}	8.35×10^{-7}	8.07×10^{-7}	8.00×10^{-7}	7.75×10^{-7}	4.98×10^{-11}	1.58×10^{-21}
$[H_2W_{12}O_{42}^{10-}]_b$	6.12×10^{-4}	1.31×10^{-3}	1.51×10^{-3}	1.62×10^{-3}	1.65×10^{-3}	1.71×10^{-3}	1.60×10^{-3}	1.57×10^{-3}	1.48×10^{-3}	6.09×10^{-12}	6.09×10^{-33}
$[H_2W_{12}O_{40}^{6-}]_b$	1.70×10^{-17}	3.63×10^{-20}	4.19×10^{-21}	1.13×10^{-23}	8.49×10^{-28}	1.89×10^{-28}	4.44×10^{-30}	4.36×10^{-31}	2.59×10^{-32}	1.40×10^{-45}	0.00
$[H_3W_{12}O_{42}^{9-}]_b$	9.35×10^{-4}	3.56×10^{-4}	2.31×10^{-4}	5.54×10^{-5}	5.15×10^{-6}	3.69×10^{-6}	1.37×10^{-6}	7.59×10^{-7}	3.57×10^{-7}	9.30×10^{-17}	2.94×10^{-39}
$[H_4W_{12}O_{42}^{8-}]_b$	2.54×10^{-4}	1.72×10^{-5}	6.26×10^{-6}	3.37×10^{-7}	2.89×10^{-9}	1.42×10^{-9}	2.10×10^{-10}	6.51×10^{-11}	1.54×10^{-11}	2.52×10^{-22}	0.00
$[H_5W_{12}O_{42}^{7-}]_b$	2.68×10^{-6}	3.22×10^{-8}	6.60×10^{-9}	7.95×10^{-11}	6.12×10^{-14}	2.11×10^{-14}	1.24×10^{-15}	2.17×10^{-16}	2.57×10^{-17}	2.66×10^{-29}	0.00

[a] The concentrations are expressed in mol dm^{-3} $W^{(vi)}$ and correspond to the plateau of the respective isotherm.

place almost exclusively through surface reaction of the WO_4^{2-} ions with one or two surface hydroxyls resulting, respectively, to a charged and uncharged surface $W^{(vi)}$ species.

As we shall see in the second article of the series (14), the mechanism of deposition of the $W^{(vi)}$ species on the γ-alumina surface established in the present work and mainly the variation of the concentration of each of the $W^{(vi)}$ species formed on the γ-alumina surface will prove to be very useful in explaining the structure, the texture, and the activity of the $W^{(vi)}/\gamma$-Al_2O_3 catalysts prepared by equilibrium deposition filtration in the pH range studied in the present work. As we shall see the surface structure of these catalysts strongly depends on the deposition mechanism.

The Factors that Determine the Extent of Deposition

In order to explain the observations mentioned in the previous section we must recall Eq. [20], which describes the deposition of a $W^{(vi)}$ species$_i$.

Careful observation of Fig. 5 clearly shows that in the pH range 10–5 the deposition takes place exclusively through deposition of the monomeric WO_4^{2-} species. This is mainly due to the fact that in this pH range the concentration in the bulk solution of the WO_4^{2-} ions is considerably higher than the concentration of the polymeric $W^{(vi)}$ species$_j$ and of the HWO_4^- species as well (see Table 3). Another very important factor that favors the deposition of the tungsten through the WO_4^{2-} ions is related to the amount $\exp(F|z_i|\Psi_{IHP}/RT)$ (see Eq. [20]). As negatively charged species are located in the lHP, the charge, and therefore the Ψ_{IHP}, is negative even at relatively low pH values where the surface charge is positive. Therefore, the value of the aforementioned amount decreases dramatically as $|z_i|$ increases, bringing about a decrease of the concentration of the species$_i$ in the IHP and then, through Eq. [20], in the final state. This simply describes the fact that the deposition of species with relatively high negative charge on a negatively charged plane is quite difficult. This is the main reason that the equilibria, which involve polymeric $W^{(vi)}$ species with z_i higher than 5, do not practically contribute to the whole deposition, although the K_i and b_i values favor their deposition. In fact, the values of K_i, being proportional to the protonation constants, favor the deposition of a polymeric species. The same is true for the b_i, the values of which increase with the number of bonds W–O and W=O and the absolute value of charge. However, the decrease in the amount $\exp(F|z_i|\Psi_{IHP}/RT)$ cannot be compensated by the increase in the K_i and in the exponential factor containing b_i even in pH lower than 5, where the bulk concentration of the polymeric species is comparable with that of the WO_4^{2-} ions. Only the polymeric species with the lowest charge $[HW_6O_{20}(OH)_2^{5-}]$ contribute to the whole deposition at very low pH where the bulk concentration is quite high (see Table 3).

The main reason for the negligible extent of deposition of the HWO_4^- species is its quite low concentration (see Table 3) in the bulk solution as well as the relatively low value of K_i and b_i.

The interesting observation that in the pH range 10–6 deposition takes place exclusively by reaction with the AlOH groups is attributed to the fact that in this pH range the concentration of the $AlOH^f$ groups is considerably higher than the concentration of the $AlOH_2^{f+}$ groups. In contrast, in the pH range 5–3.5 the protonated surface hydroxyl groups predominate and thus $C^f_{AlOH} < C^f_{AlOH_2^+}$ and this explains why the deposition occurs exclusively by adsorption in this pH range.

The last observation to explain is the negligible extent of the WO_4^{2-} deposition through adsorption on two adjacent surface hydroxyls ($AlOH_2^+$). Inspection of Eq. [20] shows that in this case the value of C_i is proportional to $(C^f_{AlOH_2^+})^2$, which is smaller than $C^f_{AlOH_2^+}$.

Closing this section it should be noted that it has been reported many times in the past that the deposition of the $Mo^{(vi)}$ (3, 15–22) or $W^{(vi)}$–oxo-species (2) on the γ-alumina surface favors the monomeric species (MoO_4^{2-}, WO_4^{2-}) with respect to the polymeric ones. The above considerations showed that the main reason for this selective deposition, at least for the WO_4^{2-} species. is the relatively low charge of the monomeric species and the negative value of the potential developed on the inner Helmholtz plane of the double layer.

ACKNOWLEDGMENT

Financial support to K. Bourikas from the Greek Award Granting Authority (IKY) is gratefully acknowledged.

REFERENCES

1. Karakonstantis, L., Kordulis, Ch., and Lycourghiotis, A., *Langmuir* **8**, 1318 (1992).
2. Spanos, N., and Lycourghiotis, A., *J. Chem. Soc. Faraday Trans.* **89**, 4101 (1993).
3. Spanos, N., and Lycourghiotis, A., *J. Catal.* **147**, 57 (1994).
4. Spanos, N., Slavov, S., Kordulis, Ch., and Lycourghiotis, A., *Langmuir* **10**, 3134 (1994).
5. Faughnan, J., "SURFEQL. An Interactive Code for the Calculation of Chemical Equilibria in Aqueous Systems," W. K. Keck Laboratories 138-78. California Institute of Technology, Pasadena, CA, 1981.
6. Contescu, C., Hu, J., and Schwarz, A. J., *J. Chem. Soc. Faraday Trans.* **89**, 4091 (1993).
7. Contescu, C., Jagiello, J., and Schwarz, A. J., *Langmuir* **9**, 1754 (1993).
8. Contescu, C., Contescu A., and Schwarz, A. J., *J. Phys. Chem.* **98**, 4327 (1994).
9. Contescu, C., Contescu, A., Schramm, G., Sato, R., and Schwarz, A. J., *J. Colloid Interface Sci.* **165**, 66 (1994).
10. "Critical Stability Constants," Smith, R. M., and Martell, A. E., Eds., Vol. 4. Plenum, New York, 1981.
11. Vordonis, L., Koutsoukos, P. G., and Lycourghiotis, A., *J. Catal.* **98**, 296 (1986).
12. Vordonis, L., Koutsoukos, P. G., and Lycourghiotis, A., *J. Catal.* **101**, 186 (1986).

13. Bourikas, K., Matralis, H. K., Kordulis, Ch., and Lycourghiotis, A., *J. Phys. Chem.*, in press.
14. Karakonstantis, L., Matralis, H. K., Kordulis, Ch., and Lycourghiotis, A., *J. Catal.* **162**, (1996).
15. Spanos, N., Vordonis, L., Kordulis, Ch., and Lycourghiotis, A., *J. Catal.* **124**, 301 (1990).
16. Iannibello, A., Marengo, S., Trifiro, F., and Villa, P. L., *in* "Proceedings, 2nd Int. Symp. on Scientific Basis for the Preparation of Heterogeneous Catalysts," Paper A5. Louvain La Neuve, Belgium, 1978.
17. Iannibello, A., and Mitchell, P. C. H., *in* "Proceedings, 2nd Int. Symp. on Scientific Basis for the Preparation of Heterogeneous Catalysts," Paper E2. Louvain La Neuve. Belgium, 1978.
18. Jeziorowski, H., and Knözinger, H., *J. Phys. Chem.* **83**, 1166 (1979).
19. Luthra, N. P., and Cheng, W. C., *J. Catal.* **107**, 154 (1987).
20. Knözinger, H., and Jeziorowski, H., *J. Phys. Chem.* **82**, 2002 (1978).
21. Medema, J., Van Stam, C., de Beer, V. H. J., Konings, A. J. A., and Koningsberger, D. C., *J. Catal.* **53**, 386 (1978).
22. Sonnemans, J., and Mars, P., *J. Catal.* **31**, 209 (1973).